

Modelling the seasonal CO₂ uptake by land vegetation using the global vegetation index

By MATTHIAS LÜDEKE, ALEX JANECEK and GUNDOLF H. KOHLMAIER, *Institut für Physikalische und Theoretische Chemie, Niederurseler Hang, D-6000 Frankfurt 50, Germany*

(Manuscript received 4 December 1989; in final form 9 October 1990)

ABSTRACT

An algorithm is developed to calculate the seasonal carbon exchange flux between the living parts of the vegetation and the atmosphere by using monthly time series of NDVI satellite data, air temperature and photosynthetically active radiation. The algorithm is based on already-existing models of the optical and physiological properties of the plant cover, introducing the concept of a seasonally variable green cover and considering some primary plant processes driven by climatic variables. The resulting carbon flux is compared to fluxes obtained by simpler models for one example pixel in Northern Germany during a period of 2 years, showing significant differences in timing and shape. In addition, the seasonal carbon exchange rate measured for beech trees is compared with the corresponding flux derived from the proposed model.

1. Introduction

The AVHRR (advanced very high resolution radiometer) aboard the NOAA 7 satellite measures the reflectance a_i in different channels “ i ”, i.e. the ratio between incident solar and reflected terrestrial electromagnetic radiation in different wave length bands.

The NDVI (normalized difference vegetation index) is defined as the following combination of the near infrared ($i = N$, λ : 725–1100 nm) and the visible red ($i = R$, λ : 580–680 nm) channel:

$$\text{NDVI} = \frac{a_N - a_R}{a_N + a_R} \quad (1)$$

It is designed to be a good measure of the photosynthetic capacity of the vegetation (Tucker and Sellers, 1986). Various authors used this NDVI concept in order to derive the seasonal carbon sink function of the terrestrial biota on a global scale (Fung et al., 1987; Heimann and Keeling, 1989). Their rather heuristic methods of correlating the NDVI directly to the net primary production (NPP) are compared with a more complex approach in which known mechanisms concerning the reflectance of the plant canopy/soil

system and the dependence of photosynthesis and autotrophic respiration on radiation and temperature are accounted for.

2. Interpretation of the NDVI

A mechanistic interpretation of the interaction between the considered electromagnetic radiation and the vegetation canopy reveals that the NDVI is primarily correlated to the leaf area index, LAI (Sellers, 1985); therefore we start with the discussion of the relation LAI(NDVI). As a basis for its calculation we take the twostream radiation model of Tucker and Sellers (1986), in which a canopy with horizontal leaves and the equivalence of leaf reflectance and transmission coefficients is assumed. For the reflectance a_i of the canopy in a defined channel “ i ” they obtained:

$$a_i(\text{LAI}) = \frac{u - v \exp(-2k \cdot \text{LAI})}{w - z \exp(-2k \cdot \text{LAI})} \quad (2)$$

with u , v , w , z and k being constants with values determined by different combinations of the scattering coefficient of leaves, ω_i , and the soil reflectance, ρ_i , for the respective channel $i = N$ or R .

The scattering coefficient ω denotes the fraction of incident radiation which is either reflected or transmitted by a single leaf. For the explicit dependence of these constants on the measurable optical parameters of leaves and soil see Appendix A. Eq. (2) has the following properties: for LAI = 0, a_i is equal to the soil reflectance ρ_i and for LAI $\rightarrow \infty$ a_i approaches a constant value. It can be shown that for the channels used in the NDVI with values for ω_i and ρ_i within the measured range (Table 1a) a constant value for a_i is reached at LAI values in the neighbourhood of 3 (Tucker and Sellers, 1986). Inserting eq. (2) into eq. (1) we obtain:

$$\text{NDVI(LAI)} = \frac{a_N(\text{LAI}) - a_R(\text{LAI})}{a_N(\text{LAI}) + a_R(\text{LAI})} \quad (3)$$

By numerical inversion, this relation allows one to calculate the LAI course from the NDVI data for given values of ω_N , ω_R , ρ_N and ρ_R . The use of eq. (3) implies a homogeneous canopy in the pixel

area, assuming that even at lowest LAI values no bare soil is detected by the satellite radiometer which leads to some shortcomings.

As a consequence of the properties of $a_N(\text{LAI})$ and $a_R(\text{LAI})$ mentioned above, changes in LAI for LAI > 3 cannot be resolved by the received NDVI signal. Nevertheless, time series of the NDVI for, e.g., Europe show a strong fluctuation of the year to year maximum values, which in this range cannot be explained as caused by atmospheric perturbations (Blümel et al., 1988). Ecological data (e.g., Reichle, 1981) indicate that the seasonal vegetation always reaches a maximum LAI significantly above 3, at least in the temperate zone. From this follows that the observed interannual variations of the maximum NDVI cannot be caused by variations in maximum LAI.

Further inspection of the maximum annual NDVI reveals that seldom a value of 0.6 is exceeded, although from the homogeneous canopy model (eq. 3) an NDVI value of about 0.8 for LAI $\gg 3$ would be expected, if reasonable

Table 1. *Parameter values*

(a) parameter ranges compiled from Blümel et al. (1988), Tucker and Sellers (1986), Gausman (1974), Baldocchi et al. (1985)

scattering coefficients of leaves	ω_N	0.66–0.93
	ω_R	0.15–0.27
soil reflectances	ρ_N	0.15–0.32
	ρ_R	0.12–0.26

(b) average parameter values used in the example calculations:

scattering coefficients	ω_N	0.85
	ω_R	0.17
soil reflectances	ρ_N	0.30
	ρ_R	0.20
LAI, where max. green cover is reached	LAI _{max}	6

(c) parameter values for the calculation of f_{NPP} (Janecek et al., 1989):

Michaelis-Menten constant	K_{PAR}	150 W m ⁻²
light attenuation coefficient	k	0.13
activation energy photosynthesis	$\Delta H_{\#}$	4.85 · 10 ⁴ J mol ⁻¹
activation energy degradation	ΔH_1	1.76 · 10 ⁵ J mol ⁻¹
entropy of degradation	ΔS	5.57 · 10 ² J mol ⁻¹ K ⁻¹
fitting parameters respiration	θ	0.06 K ⁻¹
	τ	317 K
partition factors respiration	α	0.25
	β	0.25

parameter values are used. In Table 1a parameter ranges are given, which reflect the specific vegetation/soil properties for the encountered range of water contents.

Both contradictions can be avoided by considering a non homogeneous structure of the pixel area. Given the pixel extent (approximately 15×15 km) it is clear that generally a considerable area fraction is not vegetated (water, desert, urban areas, etc.). We define the ratio between maximally

vegetated area and the pixel area as the maximum green cover, σ_{max} . It can be obtained from the annual NDVI maximum value, $NDVI_{max}$, using the fact that the maximum LAI exceeds 3 considerably, i.e., the corresponding values of a_i are independent of the LAI, such that σ_{max} can be expressed as a function of the optical properties and $NDVI_{max}$:

$$\sigma_{max} = \sigma_{max}(NDVI_{max}, \rho_N, \rho_R, \omega_N, \omega_R). \quad (4)$$

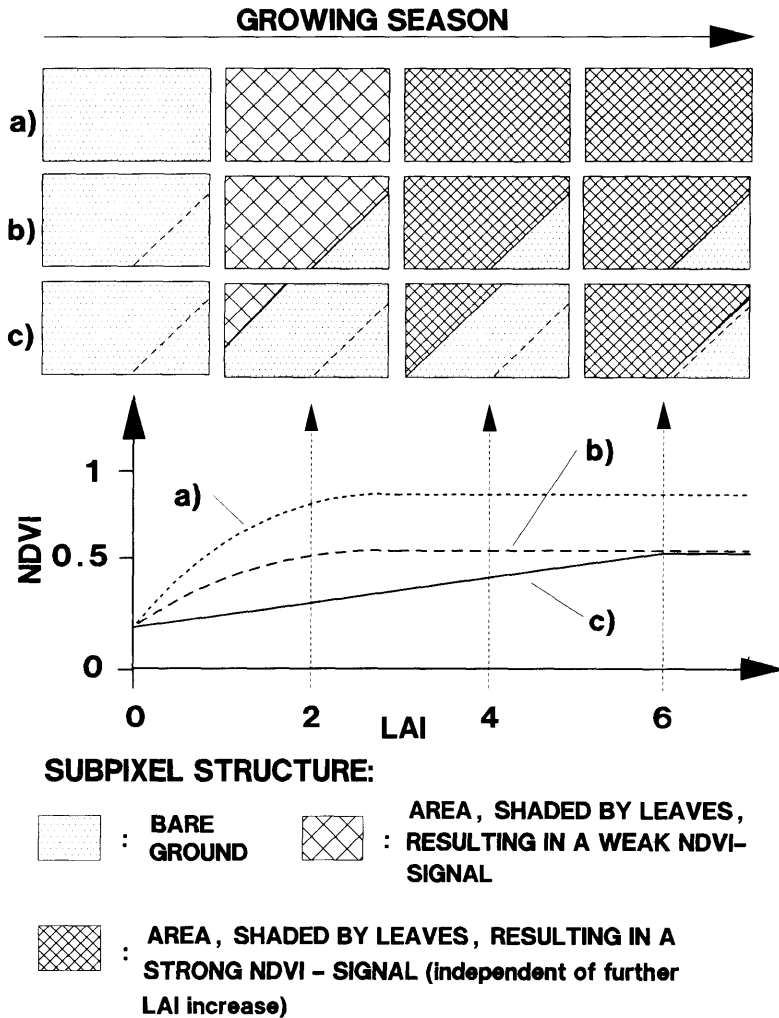


Fig. 1. Illustration of different hypotheses on subpixel structure with the resulting qualitative NDVI(LAI), as seen from the satellite: (a) homogeneous green cover $\sigma_{max} = 1$ (eq. 3); (b) constant vegetated fraction $\sigma_{max} < 1$ (eq. 5); (c) LAI dependent vegetated fraction $\sigma(LAI)$ (eq. 7).

With the assumption of a partial green cover, the spatially integrated NDVI signal of one pixel results in the following modification of eq. (3):

$$NDVI(LAI) = \frac{\{\sigma_{max}[a_N(LAI) - a_R(LAI) - \rho_N + \rho_R] + \rho_N - \rho_R\}}{\{\sigma_{max}[a_N(LAI) + a_R(LAI) - \rho_N - \rho_R] + \rho_N + \rho_R\}} \quad (5)$$

The explicit formulation of eq. (4) and derivations of eq. (4) and (5) are given in Appendix B.

In Fig. 1 (case a), pixel areas with a homogeneous canopy structure for different LAI values are shown, the corresponding NDVI(LAI) according to eq. (3) is plotted qualitatively below. The nonhomogeneous subpixel structure is visualized schematically in Fig. 1 (case b), together with the resulting NDVI(LAI) course, according to eq. (5). We would like to emphasize that the fraction of vegetated area can be distributed arbitrarily in the pixel. It is seen that in case b NDVI(LAI) reaches a lower constant value.

The interannual change in the maximum NDVI can be explained now as caused by interannual variations of the green cover, for it may vary considerably according to land use practises and climatic impact in the pixel area.

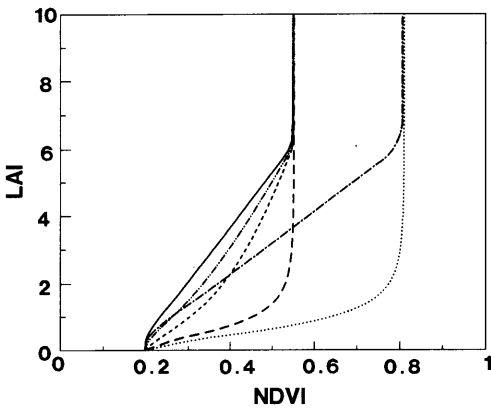


Fig. 2. LAI(NDVI) calculated with parameters from Table 1b. Using a linear $\sigma(LAI)$ relation: dotted line—constant green cover $\sigma_{max} = 1$; long dashed line—constant green cover $\sigma_{max} = 0.55$; chained line—variable green cover $\sigma(LAI)$ with $\sigma_{max} = 1$; full line—variable green cover $\sigma(LAI)$ with $\sigma_{max} = 0.55$. Using a non-linear $\sigma(LAI)$ relation: dotted chain line—variable green cover, $\sigma_{max} = 1$, $n = 0.75$; short dashed line—variable green cover, $\sigma_{max} = 0.55$, $n = 0.5$.

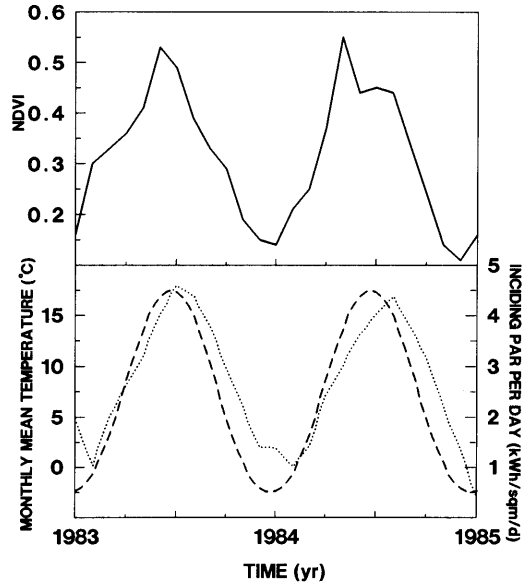


Fig. 3. Measured monthly NDVI (full line), monthly mean temperature (dotted line) and calculated daily incident PAR energy (dashed line) at 53.2°N, 7.3°E (Northern Germany).

Despite a better description of some observations by the introduction of σ_{max} , there is still another inconsistency with ecological ground truth. Adjusting the green cover parameter σ_{max} to get a reasonable maximum LAI leads to unrealistically steep peaks in the LAI time course during the year, which is in contradiction to ecological observations (e.g., Madgewick, 1968), stating that a LAI value significantly greater than 3 is maintained for at least three months in the temperate zone. The reason for the steep LAI peaks becomes clear by comparing the example NDVI time course in Fig. 3 and the long dashed line in Fig. 2: while the maximum NDVI corresponds to a reasonable LAI value of about 6, in the months before and after the peak values smaller than 3 are obtained.

At the same time it is quite plausible that generally the green cover varies with the developmental stage of the vegetation, i.e., the pixel area is more and more covered by the upgrowing vegetation as illustrated in Fig. 1 (case c), until σ_{max} , the maximum vegetated area fraction, is reached. On account of this fact we introduce a time dependent green cover $\sigma(LAI)$.

As for many developments of biological systems we assume here that for the shape of $\sigma(\text{LAI})$ a general allometric relation is valid:

$$\sigma(\text{LAI}) = \begin{cases} \sigma_{\max}(\text{LAI}/\text{LAI}_{\max})^n & \text{for } 0 \leq \text{LAI} \leq \text{LAI}_{\max} \\ \sigma_{\max} & \text{for } \text{LAI} > \text{LAI}_{\max} \end{cases} \quad (6)$$

Here, LAI_{\max} denotes the LAI value where the maximum green cover, σ_{\max} , is reached and the exponent $n \geq 0$ is a parameter, determining the shape of the curve. Dependent on the value of n , eq. (6) yields a constant green cover ($n = 0$), a fast increase of σ at low LAI values ($0 < n < 1$), a linear relationship ($n = 1$) or, rather unlikely, a fast increase of σ at LAI values near LAI_{\max} . With $\sigma(\text{LAI})$ defined, eq. (5) now takes the form:

$$\text{NDVI}(\text{LAI}) = \frac{\{\sigma(\text{LAI})[a_N(\text{LAI}) - a_R(\text{LAI}) - \rho_N + \rho_R] + \rho_N - \rho_R\}}{\{\sigma(\text{LAI})[a_N(\text{LAI}) + a_R(\text{LAI}) - \rho_N - \rho_R] + \rho_N + \rho_R\}} \quad (7)$$

To estimate the parameters in eq. (6), we used data of Huete et al. (1985) for cotton plantations (*Gossypium hirsutum*); the evaluation of this data set (documented in Appendix C) yields that the relationship between green cover and LAI is linear ($n = 1$), the correlation coefficient being $r = 0.99$, and that the green cover of 100% ($\sigma = 1$) is reached at maximum LAI.

Due to the lack of more data, we preliminarily assume a linear relation for all relevant vegetation types with a pronounced seasonality; anyhow, this approximation does not detract from the idea itself to correct the calculation of $\text{NDVI}(\text{LAI})$ by a seasonally varying green cover.

The qualitative course of NDVI with respect to LAI according to eq. (7) is plotted in the lower part of Fig. 1 (case c). It is seen that $\text{NDVI}(\text{LAI})$ is now nearly linear up to the value of LAI , at which σ_{\max} is reached. In this paper we consider as an example deciduous forest ecosystems with an average maximum LAI of 6 which we set equal to LAI_{\max} . In Fig. 2, $\text{LAI}(\text{NDVI})$ for the three discussed cases is plotted, using the parameters from Table 1b, assumed to be representative for the deciduous forest ecosystem under average humidity conditions. The difference between the

$\text{LAI}(\text{NDVI})$ with a constant green cover σ_{\max} (eq. 5) and a $\text{LAI}(\text{NDVI})$ derived using the presented concept of the growth stage dependent $\sigma(\text{LAI})$ (eq. 7) is appreciable. It can be seen clearly that changes for $\text{LAI} \gg 3$ can be resolved from the NDVI data, due to a decreasing fraction of bare soil during the vegetation period; the curves coincide from the LAI value on, where full green cover is reached. Furthermore, the short-dashed and dotted-chain curve show the sensitivity of eq. (7) on deviations from linearity in the $\sigma(\text{LAI})$ relation (eq. (6), $n = 0.75$ and $n = 0.5$) with the result that the property of resolving LAI changes for LAI greater than 3 is preserved.

While the influence of a fixed green cover has been already discussed by some authors (e.g., Sellers, 1985), to our knowledge a growth stage dependent green cover has not been used yet in order to correct the LAI calculation by the two stream radiation model.

3. Calculation of the carbon fluxes

For the calculation of the carbon fluxes, the model of Janecek et al. (1989) is used, describing the seasonal carbon dynamics in deciduous forests. According to their model we consider two carbon fluxes connected to the living biomass, namely photosynthetic production and autotroph respiration of green and woody plant parts.

The LAI calculated by eq. (7) together with surface air temperature, T , and incident photosynthetically active radiation, PAR , is used to determine the effective assimilation rate, EAR , of the vegetation, i.e., the total carbon uptake minus photorespiration in the pixel area, where the light dependence follows a Monsi-Saeki-type function:

$$\text{EAR}(\text{LAI}, T, \text{PAR}) = Ag(T) \times \ln \frac{K_{\text{PAR}} + \text{PAR}}{K_{\text{PAR}} + \text{PAR} e^{-k \text{LAI}}} \sigma(\text{LAI}). \quad (8)$$

K_{PAR} : specific Michaelis-Menten constant, k : light extinction coefficient of a single leaf layer, A : normalization constant; with

$$g(T) = \frac{T e^{\Delta H \# / RT}}{1 + e^{-\Delta H_1 / RT} e^{\Delta S / R}} \quad (9)$$

T : temperature in Kelvin, $\Delta H \#$: activation energy

of photosynthesis, ΔH_1 : activation energy of degradation, ΔS : entropy of degradation, R : gas constant.

The consideration of precipitation has been excluded due to the complexity of the subject, although it is recognized that soil humidity may influence both the assimilation rate and soil reflectance considerably; it shall be treated in a future publication.

Because of different dynamics, the respiration is calculated separately for the green and woody biomass. For dark respiration of the photosynthetically active parts of plants we used

$$\text{RESG} = \begin{cases} Bf(T) \text{ LAI } \sigma(\text{LAI}) & \text{for } \text{PAR}(t) < \text{PAR}_{\min} \\ 0 & \text{otherwise} \end{cases} \quad (10)$$

while the respiration of the woody parts is correspondingly

$$\text{RESG} = Cf(T) \quad (11)$$

with

$$f(T) = \exp[\theta(T - \tau)]. \quad (12)$$

θ, τ : fitting parameters for the quasi-Arrhenius type function. Dark respiration is suppressed when PAR reaches the threshold PAR_{\min} (eq. 10). To a first approximation, the standing woody biomass is assumed to be constant, and in eq. (11) no dependence of $\sigma(\text{LAI})$ is considered.

In order to obtain normalized fluxes, we consider the climatic variables and the NDVI-course of a reference year and determine the constants A, B and C from the following equations:

$$\int_{\text{ref. year}} \text{EAR}(\text{PAR}, T, \text{NDVI}) dt = 1, \quad (13a)$$

$$\int_{\text{ref. year}} \text{RESG}(\text{PAR}, T, \text{NDVI}) dt = 1, \quad (13b)$$

$$\int_{\text{ref. year}} \text{RESR}(T) dt = 1. \quad (13c)$$

The normalized net carbon flux between the

atmosphere and the living vegetation, $f_{\text{NPP}}(t)$, is calculated by:

$$f_{\text{NPP}}(t) = \{ \text{EAR}(t) - \alpha \text{RESG}(t) - \beta \text{RESR}(t) \} / \{ 1 - \alpha - \beta \}. \quad (14)$$

α and β denote the fractions of the annual EAR, which are respired by green and woody biomass, respectively. Using eqs. (13a)–(13c) integration of eq. (14) yields:

$$\int_{\text{ref. year}} f_{\text{NPP}}(t) dt = 1. \quad (15)$$

Thus, with $f_{\text{NPP}}(t)$ determining the time course, the absolute carbon flux between the living biomass and the atmosphere, $F_{\text{NPP}}(t)$ is given by:

$$F_{\text{NPP}}(t) = f_{\text{NPP}}(t) \sigma_{\max} I_{\text{Pixel}} \text{NPP}, \quad (16)$$

where I_{Pixel} is the pixel area and NPP the typical net primary productivity per year of the monitored vegetation type. The information on vegetation type and the corresponding NPP is contained e.g. in the vegetation map of Matthews (1983).

4. Results

As an example, we chose a location with a pronounced seasonality. An average of 15 neigh-

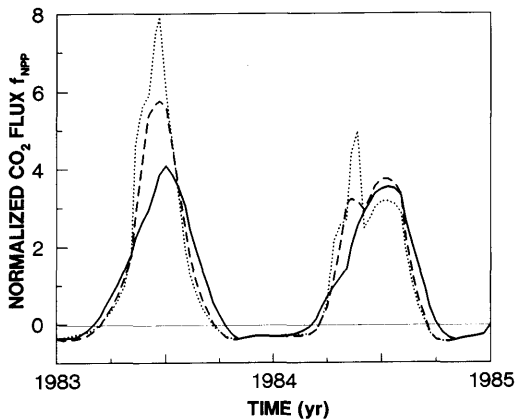


Fig. 4. Normalized CO₂ flux between vegetation and atmosphere calculated by eqs. (8)–(14) with: LAI(NDVI) according to eq. (3) (dashed line); LAI(NDVI) as given in eq. (5) with constant σ_{\max} from eq. (4) (dotted line); LAI(NDVI) according to eq. (7) with LAI dependent green cover (full line).

bouring NDVI pixels in a forested area of North Germany, derived by the maximum sample method, for the years 1983 and 1984 (Esser, 1989), along with a temperature record for the same location and light intensity calculated by a model of Richter (1985) was used to determine the normalized $f_{NPP}(t)$ flux. The input data is displayed in Fig. 3. The parameter set shown in Table 1b–c was used.

The influence of the LAI(NDVI) calculation procedure on the resulting $f_{NPP}(t)$ is illustrated in Fig. 4, demonstrating that the NPP flux is highly sensitive to the different LAI(NDVI) relations employed.

In Fig. 5, $f_{NPP}(t)$ is compared to the carbon uptake rates calculated by the two methods used by Fung et al. (1987):

$$f_{NPP}^{F1}(t) \sim (NDVI - 0.1), \tag{17}$$

$$f_{NPP}^{F2}(t) \sim \{\exp[10(NDVI - 0.1)] - 1\}, \tag{18}$$

and the approach of Heimann and Keeling (1989):

$$f_{NPP}^{H1}(t) \sim (SR - 1.05) PAR, \tag{19}$$

with $SR = (1 + NDVI)/(1 - NDVI)$. All curves are normalized to the reference year 1983 and calculated with the same time series input. It can

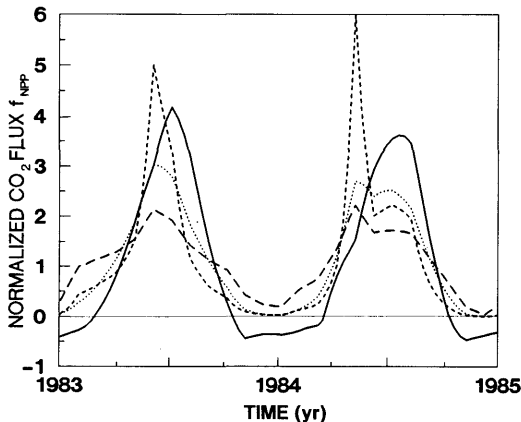


Fig. 5. Comparison of the normalized f_{NPP} flux as calculated by the authors (eqs. (7–14), full line) with the corresponding fluxes calculated according to: Fung et al. (1987), linear dependence on NDVI (eq. (17), long-dashed line) and exponential dependence on NDVI (eq. (18), short dashed line); Heimann and Keeling (1989) (eq. (19), dotted line).

be seen that by introduction of the dependence on temperature and PAR a f_{NPP} time course is obtained, which differs clearly from that derived by the simpler algorithms. Furthermore a clear separation of the vegetation period from the dormancy period is achieved by negative f_{NPP} values in winter, due to the excess autotrophic respiration.

Measurements of the seasonal CO_2 exchange between natural ecosystems and the atmosphere are very sparse. In order to assess the results we compared seasonal measurements of the foliage carbon exchange rate (f_{CER}) of *Fagus silvatica* in Northern Germany (Schulze, 1970) with the average time course of the f_{CER} as generated by the proposed algorithm

$$f_{CER}(t) = \{EAR(t) - \alpha RESG(t)\} / \{1 - \alpha - \beta\}. \tag{20}$$

The measurements were performed in 1969, a year without extreme climatic events, such that the data seem appropriate for a qualitative test of our results. In Fig. 6 a fairly good agreement in shape and phase can be observed. Higher values of the calculated f_{CER} in early spring may be caused by the herb layer which is photosynthetically active before the shoots of trees start and which is not considered in the ground measurements.

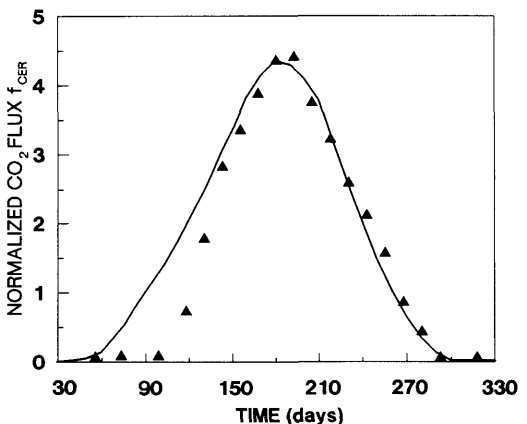


Fig. 6. Comparison of the carbon exchange rate of *Fagus silvatica* in Northern Germany measured by Schulze (1970) (triangles) with the arithmetic average of two seasonal f_{CER} courses calculated with the proposed algorithm (eqs. (7–13c), 20) for the years 1983 and 1984.

5. Conclusions

In summary, we observe that the calculation of the seasonal uptake of carbon by vegetation from the global vegetation index is highly dependent on the interpretation of the NDVI, taken here as correlated primarily to the leaf area index (LAI) of the vegetation. In order to obtain realistic time courses of the LAI as a function of the measured NDVI, the two stream radiation model (Tucker and Sellers, 1986) had to be corrected by the introduction of a variable green cover $\sigma(\text{LAI})$. Incorporation of mechanisms accounting for the influence of climatic variables on the net primary production led to significantly different results, when compared to heuristic approaches. As important ecological findings are accounted for in the LAI(NDVI) derivation as well as in the calculation of the carbon flux connected to it, the results seem trustworthy; furthermore a comparable measured flux is reproduced satisfactorily (local verification). Despite of its relative complexity, the proposed algorithm does not present any serious problems for its application on a global scale; actually we perform calculations of the carbon exchange of the whole global vegetation cover with the atmosphere. In general most of the model parameters should vary with the vegetation type in determinable ranges; as a first approximation averaged parameter values are used globally, as long as only sparse data is available. In the future, the global applicability of the algorithm will be tested by adding a model for heterotrophic respiration and atmospheric transport and comparing the resulting fluxes with detrended seasonal atmospheric concentration measurements.

6. Acknowledgements

The authors thank the Bundesministerium für Forschung und Technologie for financial support. Furthermore, thanks are expressed to Dr. Martin Heimann for helpful discussions and to our colleagues Günther Benderoth and Jürgen Kindermann for their considerable help and support.

7. Appendix A

The constants u , v , w , z and k used in eq. (2) depend on the scattering coefficient of leaves,

ω_i , and the soil reflectance, ρ_i , for a specified channel i :

$$k = (1 - \omega_i)^{1/2}, \tag{A1}$$

$$u = \omega_i, \tag{A2}$$

$$w = 2(1 - \frac{1}{2}\omega_i + k), \tag{A3}$$

$$v = \omega_i \frac{(1 - \frac{1}{2}\omega_i + k) - \omega_i/(2\rho_i)}{(1 - \frac{1}{2}\omega_i - k) - \omega_i/(2\rho_i)}, \tag{A4}$$

$$z = 2(1 - \frac{1}{2}\omega_i - k)/\omega_i v \tag{A5}$$

8. Appendix B

Eqs. (4) and (5) are based on the assumption that the pixel area is subdivided in a part which can be described by the reflectance of a homogeneous canopy (eq. 3) and another part with reflection properties of bare ground. Thus, one obtains for the effective reflectance, a_i^{eff} , of the whole pixel in the channel “ i ”:

$$a_i^{\text{eff}}(\text{LAI}) = \sigma_{\text{max}} a_i(\text{LAI}) + (1 - \sigma_{\text{max}}) \rho_i. \tag{B1}$$

To calculate the resulting NDVI signal, we insert eq. (B1) into eq. (1):

$$\text{NDVI}(\text{LAI}) = \frac{a_{\text{N}}^{\text{eff}}(\text{LAI}) - a_{\text{R}}^{\text{eff}}(\text{LAI})}{a_{\text{N}}^{\text{eff}}(\text{LAI}) + a_{\text{R}}^{\text{eff}}(\text{LAI})}, \tag{B2}$$

and obtain

$$\text{NDVI}(\text{LAI}) = \frac{\{\sigma_{\text{max}}[a_{\text{N}}(\text{LAI}) - a_{\text{R}}(\text{LAI})] + (1 - \sigma_{\text{max}})[\rho_{\text{N}} - \rho_{\text{R}}]\}}{\{\sigma_{\text{max}}[a_{\text{N}}(\text{LAI}) + a_{\text{R}}(\text{LAI})] + (1 - \sigma_{\text{max}})[\rho_{\text{N}} + \rho_{\text{R}}]\}} \tag{B3}$$

Rearrangement of the terms on the right-hand side of eq. (B3) yields eq. (5).

For the derivation of eq. (4), we used the relation

$$\text{NDVI}_{\text{max}} = \lim_{\text{LAI} \rightarrow \infty} \text{NDVI}(\text{LAI}), \tag{B4}$$

which is motivated by the fact that the maximum annual NDVI, NDVI_{max} , coincides with $\text{LAI} \gg 3$. For $\text{LAI} \rightarrow \infty$, eq. (2) becomes

$$a_{i,\max} = \lim_{\text{LAI} \rightarrow \infty} a_i(\text{LAI})$$

$$= \frac{\omega_i}{2(1 - \frac{1}{2}\omega_i + (1 - \omega_i)^{1/2})}. \quad (\text{B5})$$

and with eqs. (B3), (B4) and (B5) we obtain

$$\text{NDVI}_{\max} = \frac{\{\sigma_{\max}[a_{\text{N},\max} - a_{\text{R},\max}] + (1 - \sigma_{\max})[\rho_{\text{N}} - \rho_{\text{R}}]\}}{\{\sigma_{\max}[a_{\text{N},\max} + a_{\text{R},\max}] + (1 - \sigma_{\max})[\rho_{\text{N}} + \rho_{\text{R}}]\}}. \quad (\text{B6})$$

Solving eq. (B6) for σ_{\max} , yields the explicit form of eq. (4):

$$\sigma_{\max} = \frac{\{(1 - \text{NDVI}_{\max})\rho_{\text{N}} - (1 + \text{NDVI}_{\max})\rho_{\text{R}}\}}{\{(1 - \text{NDVI}_{\max})(\rho_{\text{N}} - a_{\text{N},\max}) - (1 + \text{NDVI}_{\max})(\rho_{\text{R}} - a_{\text{R},\max})\}}. \quad (\text{B7})$$

9. Appendix C

Green cover and leaf area index as measured by Huete et al. (1984) in a cotton field:

Day of year	green cover (%)	leaf area index
170	0	0
196	20	0.5
198	25	0.7
208	40	1.0
215	55	1.5
217	60	-
223	75	2.8
228	90	-
235	95	3.3
242	100	3.6

REFERENCES

- Baldocchi, D. D., Hutchinson, B. A., Matt, D. R. and McMillen, R. T. 1985. Canopy radiative transfer models for spherical and known leaf inclination angle distributions: a test in an oak-hickory forest. *J. Applied Ecol.* 22, 539-555.
- Blümel, K., Bolle, H.-J., Eckhardt, M., Lesch, L. and Tonn, W. 1988. *The vegetation index for Central Europe 1983-1985 (In German)*. Berlin, Institut für Meteorologie der Freien Universität Berlin, LOF 84/3, 70 p.
- Esser, G. 1989. Compilation of climatically relevant geocological data and space patterns of sensitive vegetation zones from remote sensing data (In German). *Conference Report, Statusseminar 10.1.-12.1.1989, "Klimaforschungs-programm"*, Gesellschaft für Strahlen- und Umweltforschung mbH München, Ingolstädter Landstraße 1, D-8042 Neuherberg, 231-234.
- Fung, I. Y., Tucker, C. J. and Prentice, K. C. 1987. Application of advanced very high resolution radiometer vegetation index to study atmosphere-biosphere exchange of CO₂. *J. Geophys. Res.* 92, D3, 2999-3015.
- Gausman, H. W. 1974. Leaf reflectance of near-infrared. *Photogram. Engng.* 40, 183.
- Heimann, M. and Keeling, C. D. 1989. A three-dimensional model of atmospheric CO₂ transport based on observed winds: 2. Model description and simulated tracer results. *Geophysical Monographs* 55 (American Geophysical Union), 237-275.
- Huete, A. R., Jackson, R. D. and Post, D. F. 1985. Spectral response of a plant canopy with different soil backgrounds. *Remote Sensing of Environment* 17, 37-53.
- Janecek, A., Benderoth, G., Lüdeke, M. K. B., Kindermann, J. and Kohlmaier, G. H. 1989. Model of the seasonal and perennial carbon dynamics in deciduous type forests controlled by climatic variables. *Ecol. Mod.* 49, 101-124.
- Madgwick, H. A. I. 1967. Seasonal changes in biomass and annual production of an old-field *Pinus virginiana* stand. *Ecology* 49, 149-152.
- Matthews, E. 1983. Global vegetation and land use: New high-resolution data basis for climate studies. *J. Clim. Appl. Meteorol.* 22, 474-487.
- Richter, O. 1985. *Simulation of the behaviour of ecological systems (in German)*, Weinheim, VCH Verlagsgesellschaft, 219 p.
- Reichle, D. E. 1981. *Dynamic properties of forest ecosystems. IBP 23*. Cambridge, Cambridge University Press, 683 p.
- Schulze, E.-D. 1970. The CO₂ gas exchange of the beech (*fagus silvatica* L.) as dependent on climatic factors under field conditions (in German). *Flora* (VEB Gustav Fischer Verlag, DDR-69 Jena, Villengang 2), 159, 177-232.
- Sellers, P. J. 1985. Canopy reflectance, photosynthesis and transpiration. *Int. J. Remote Sensing* 6, 1335-1372.
- Tucker, C. J. and Sellers, P. J. 1986. Satellite remote sensing of primary production. *Int. J. Remote Sensing* 7, 1395-1416.